African Journal of Environment and Natural Science Research
ISSN: 2689-9434
Volume 9, Issue 3, 2026 (pp. 95-112)
www.abjournals.org

INTEGRATED AGRO-WASTE BINARY BIOCHAR FOR HEAVY METAL REMEDIATION AND SUSTAINABLE SOIL MANAGEMENT

Sibe L.[1*], Frank O.[2], Aguomba C. C.[3], Domgbara T.[4], and Nordee B. S.[5]

[1]Biochemistry/Chemistry Technology, School of Science Laboratory Technology, University of Port Harcourt, Choba, Rivers State, P.M.B. 5323, Nigeria.

[2]Chromatography Laboratory, QAQC Department, Indorama-Eleme Petrochemicals Limited, Rivers State, Nigeria.
Email: oteiva.frank@gmail.com

[3]Oil, Gas & Chemicals Division, SGS Inspection Service, Rivers State, Nigeria.
Email: chukwudi.aguomba@sgs.com

[4]Department of Chemical Engineering, Louisiana State University, Baton Rouge.
Email: tdomgb1@lsu.edu; Tel.: +12253771080

[5]Chemistry Department, Rivers State University, Nkpolu Orowurukwu, Port Harcourt.
Email: barilugbene.nordee@ust.edu.ng; Tel.: +2348068104895

[*]Corresponding Author's Email: lebari.sibe@uniport.edu.ng, Tel.: +2347030600892

Cite this article:

Sibe L., Frank O., Aguomba C. C., Domgbara T., Nordee B. S. (2026), Integrated Agro-Waste Binary Biochar for Heavy Metal Remediation and Sustainable Soil Management. African Journal of Environment and Natural Science Research 9(3), 95-112. DOI: 10.52589/AJENSR-VZVQM4DR

Manuscript History

Received: 11 May 2026

Accepted: 15 Jun 2026

Published: 9 Jul 2026

ABSTRACT: *This research investigated the potential and effectiveness of agro-waste biochar composites derived from empty palm fruit bunch and coconut husk (EPFBB–CHB) and palm kernel shell and coconut shell (PKB–CSB) in immobilizing metals (Fe, Cu, Cr, Ni, Pb, Zn, Cd, and As) to alleviate contaminated soils. Soils were collected, air- and oven-dried, sieved, and artificially spiked to 100 mg/kg for each metal. The metal levels in soil were determined spectroscopically before and after treatments. The biochar was synthesized via pyrolysis at 500 °C, and two composites were prepared: EPFBB–CHB and PKB–CSB. Ten grams of contaminated soil were treated with 5% w/w biochar and incubated for 72 hours and characterized for surface physicochemical parameters. The findings indicated that the untreated soil exhibited significant contamination levels of Fe (160.8 ± 10.50 mg/L), Cu (166.05 ± 10.30 mg/L), Cr (153 ± 9.41 mg/L), Ni (135.35 ± 8.17 mg/L), Pb (107 ± 7.93 mg/L), Zn (158.495 ± 10.12 mg/L), Cd (163.35 ± 10.61 mg/L), and As at 0.35 ± 0.0001 mg/L (unspiked environmental concentration). Treatment-A (EPFBB-CHB) exhibited greater effectiveness in the removal of Cu, Pb, and Cd, achieving removal efficiencies of 73.35%, 85.39%, and 22.52%, respectively. In contrast, Treatment-B (PKB-CSB) demonstrated slightly higher efficiency in removing Fe, Cr, Ni, and Zn, with removal efficiencies of 97.24%, 24.47%, 84.81%, and 53.67%, respectively. The findings indicate that EPFBB–CHB was more effective for Fe, Cu, Pb, and Ni, but PKB–CSB had superior performance for Zn and Cr. Both composites effectively immobilized arsenic, while cadmium remained stable for an extended duration. Functional group analysis revealed adsorption-promoting aromatic, phenolic, and oxygenated compounds, but also indicated persistent organic pollutants, highlighting potential environmental risks. The study concludes that agro-waste biochar is a low-cost, sustainable method for reducing heavy-metal mobility in contaminated soils, and recommends optimization, repeated applications, or combined remediation strategies to achieve regulatory compliance and restore soil health in metal-contaminated soils.*

KEYWORDS: Agro-waste biochar, Bioavailability, Heavy metal immobilization, Soil health, Sustainable remediation.

Article DOI: 10.52589/AJENSR-VZVQM4DR
DOI URL: https://doi.org/10.52589/AJENSR-VZVQM4DR

INTRODUCTION

Heavy metal contamination of soils is a global environmental concern with serious implications for agricultural productivity, ecosystem stability, and human health. Worldwide, activities such as industrialization, mining, fossil fuel exploitation, intensive agriculture, and improper waste disposal have increased the release of potentially toxic metals, including cadmium (Cd), lead (Pb), chromium (Cr), nickel (Ni), copper (Cu), zinc (Zn), arsenic (As), and iron (Fe), into terrestrial environments (Ezugwu et al., 2022). These metals are non-biodegradable and persist in soils for long periods, where they disrupt soil physicochemical properties, suppress microbial activity, and accumulate in crops, thereby posing long-term risks through the food chain (Zhang et al., 2023).

In response to these challenges, global research has increasingly focused on sustainable and low-impact soil remediation technologies. Conventional methods such as excavation, soil washing, and chemical stabilization are often effective but costly, energy-intensive, and unsuitable for large agricultural lands, particularly in resource-limited settings (Ahmed et al., 2025). Consequently, attention has shifted toward environmentally friendly approaches, with biochar emerging as a promising remediation material. Biochar is a carbon-rich product obtained from the pyrolysis of biomass under limited oxygen conditions. Its high surface area, porous structure, and functional groups enable it to immobilize heavy metals through adsorption, ion exchange, and surface complexation, thereby reducing their mobility and bioavailability in soils (Sizmur et al., 2017; Yaashikaa et al., 2020).

Across Africa, soil contamination by heavy metals has intensified due to rapid urbanization, weak environmental governance, artisanal mining, oil exploitation, and unmanaged waste streams. Several studies have reported heavy metal concentrations in African agricultural soils exceeding international safety limits, raising concerns about food safety and public health (Ezugwu et al., 2022). At the same time, the continent produces large volumes of agricultural residues that are often burned or discarded, contributing to environmental degradation. The conversion of agro-wastes into biochar therefore represents a sustainable pathway for waste valorization while addressing soil contamination challenges (Abbas et al., 2021).

Nigeria, particularly the Niger Delta region, exemplifies the intersection of severe soil contamination and agricultural vulnerability. Decades of crude oil exploration, gas flaring, industrial emissions, artisanal refining, and poor waste management have resulted in widespread soil pollution (UNEP, 2011). Ogoni land has been identified as one of the most affected areas, with reported elevations of Fe, Cr, Ni, Cd, Pb, Zn, Cu, and As in agricultural soils (Zhang et al., 2023). These contaminants reduce soil fertility, impair crop performance, and increase the risk of metal accumulation in food crops, threatening rural livelihoods and food security.

Recent Nigerian studies have explored biochar derived from local agro-wastes, such as oil palm residues and coconut shells, for soil remediation. However, biochar effectiveness is highly site-specific and depends on feedstock type, soil properties, and contamination history (Mohan et al., 2014). Evidence further suggests that biochar composites produced from multiple agro-wastes may exhibit enhanced heavy metal immobilization due to synergistic physicochemical properties (Tian et al., 2025). Despite this potential, limited data exist on the performance of agro-waste biochar composites in Ogoni soils. This study therefore investigates the heavy metal remediation potential

Article DOI: 10.52589/AJENSR-VZVQM4DR
DOI URL: https://doi.org/10.52589/AJENSR-VZVQM4DR

of a biochar composite produced from empty palm fruit bunches and coconut husks in the soil of Songhai Farm, Bunu, Ogoni land, with the aim of contributing site-specific evidence for sustainable soil restoration in the Niger Delta.

MATERIALS AND METHODS

Study Design

This study was conducted using soil obtained from Songhai Farm, Bunu, located in Tai Local Government Area of Rivers State, Nigeria. Songhai Farm occupies approximately 314 hectares and lies within Ogoni land in the Niger Delta region (Onwuchekwa, 2022). Geographically, Bunu is situated at approximately 4.45°43″ N latitude and 7.14°32″ E longitude. The area experiences a humid tropical climate characterized by high annual rainfall, elevated humidity, and consistently high temperatures, conditions that influence soil chemistry and contaminant mobility.

Tai Local Government Area is bordered by Akwa Ibom State to the east, Imo and Bayelsa States to the west, Abia State to the north, and the Atlantic Ocean to the south. According to the 2006 national population census, Tai has a population of about 117,797 and covers a land area of 159 km². Agriculture and fishing are traditionally the dominant livelihoods; however, their productivity has declined due to long-term environmental degradation. The area hosts several oil wells and pipelines operated mainly by Shell Nigeria, making the soils vulnerable to contamination from petroleum-related activities (Onwuchekwa, 2022). Songhai Farm was selected because it represents an agriculturally active site within an oil-impacted region and generates substantial agro-waste suitable for biochar production.

Sample Collection, Preservation and Preparation

Sample Collection

Soil samples were collected following standard procedures to ensure representativeness and reproducibility. Surface litter, stones, and plant residues were removed prior to sampling. Topsoil samples (0–20 cm depth) were collected from multiple points across Songhai Farm using a stainless-steel auger. These soil subsamples were thoroughly mixed to form a composite sample weighing approximately 5 kg, thereby minimizing spatial variability in accordance with USEPA (2022) standard procedures.

The composite soil sample was placed in pre-cleaned polyethylene bags, properly labelled, and transported to the laboratory. In the laboratory, the soil was air-dried under shaded conditions and subsequently oven-dried at 100 °C for 24 hours. The dried soil was sieved through a 2 mm mesh to remove coarse materials and ensure homogeneity. Prepared soil samples were stored in airtight containers until further use.

Agro-waste materials, specifically empty palm fruit bunches and coconut husks, were sourced from Songhai Farm for biochar production. These feedstocks were washed with distilled water to remove adhering impurities, air-dried, oven-dried at 105 °C, and stored prior to pyrolysis.

Article DOI: 10.52589/AJENSR-VZVQM4DR
DOI URL: https://doi.org/10.52589/AJENSR-VZVQM4DR

Biochar Preparation and Characterization

Following the method adopted by Mahmoud et al. (2024), biochar was produced through pyrolysis of the prepared agro-wastes in a laboratory muffle furnace at 500 °C with a heating rate of 10 °C per minute and a residence time of 2 hours under limited oxygen conditions. After cooling, the biochar was pulverized and sieved to 2 mm. A biochar composite was prepared by thoroughly homogenizing empty palm fruit bunch biochar and coconut husk biochar.

Biochar characterization was conducted to determine properties influencing metal immobilization. Parameters such as pH, surface area, porosity, bulk density, and cation exchange capacity were determined using standard APHA (2005) methods. The study utilized GC-MS to profile the possible surface functional groups, while elemental analysis was quantified with the aid of atomic absorption spectrophotometry.

Adsorption / Remediation Experiment

Spiking of Soil Sample

To simulate heavy metal contamination, 25 g portions of the prepared soil sample were spiked with calculated masses of 4.0 mg, 4.1 mg, 11.2 mg, 7.1 mg, 12.5 mg and 11 mg analytical-grade metal salts of Lead nitrate - $Pb(NO_3)_2$, Cadmium chloride – $CdCl_2$, Copper sulfate heptahydrate – $CuSO_4 \cdot 7H_2O$, Potassium dichromate – $K_2Cr_2O_7$, Iron II sulfate heptahydrate –$FeSO_4 \cdot 7H_2O$ and Zinc sulfate heptahydrate –$ZnSO_4 \cdot 7H_2O$ to achieve a concentration of 100 mg/kg for each metal of interest using the formula:

$$Target\ Concentration\ \left(\frac{mg}{kg}\right) = soil\frac{g}{1000} \times \frac{Msalt}{Mmetal} \qquad (2.1)$$

Where *Msalt* = molarity of salt; *Mmetal* = atomic mass of metal of interest. The metals investigated included iron (Fe), chromium (Cr), nickel (Ni), cadmium (Cd), lead (Pb), zinc (Zn), and copper (Cu) introduced using the above salts. The spiked soil was thoroughly mixed to ensure uniform distribution.

Sample Digestion and Analysis

Baseline metal concentrations were determined by weighing and digesting 1 g of the spiked soil with a solution of aqua regia (HCl: HNO_3) on a hot plate inside a fume cupboard following USEPA (2022) procedures. The digests were cooled, filtered through Whatman No. 42 µm filter paper, made up to 100 mL with distilled water, and analyzed using an Agilent 500 Flame Atomic Absorption Spectrophotometer (AAS).

Sample Treatment

Ten grams (10g) of contaminated soil was properly mixed with 0.5 g of biochar composite (5% w/w) determined using the formula:

Article DOI: 10.52589/AJENSR-VZVQM4DR
DOI URL: https://doi.org/10.52589/AJENSR-VZVQM4DR

$$Biochar\ mass\ (g) = Soil\ mass\ (g) \times \frac{Amendment}{100} \qquad (2.2)$$

Where, Amendment = rate variation (g) in a conical flask. Fifty milliliters (50mL) of distilled water was added, and the mixture was incubated at ambient temperature (20–30 °C) for 72 hours with intermittent shaking to enhance contact between soil, biochar, and metal ions. After incubation, the mixture was filtered, acidified with 0.5 mL of concentrated HNO_3 to preserve the metal ions, and then analyzed for residual metal concentrations using AAS in accordance with USEPA 3015A.

Adsorption efficiency was evaluated by comparing initial and final metal concentrations using the standard removal efficiency equation.

$$Adsorption\ Efficiency\ (\%) = C_o - \frac{C_e}{C_o} \times 100 \qquad (2.3)$$

Where *Co* is the initial metal concentration, and *Ce* is the final metal concentration

Data Analysis

Descriptive statistics, charts, and measures of central tendency were applied to summarize the data. One-way Analysis of Variance (ANOVA) was used to assess significant differences between treated and untreated samples, providing a statistical basis for evaluating the remediation effectiveness of the agro-waste biochar composite.

RESULTS

A= Treatment-A (EPFBB-CHB), B= Treatment-B (PKB -CSB), A (%) & B (%) = Removal %.

Table 1: Mean concentration (±SD) of heavy metals (mg/L) in untreated and treated soil samples using different biochar composites.

S/N	Metals	Untreated	A	B	A (%)	B (%)	USEPA (2022)	SON (2015)
1	Fe	160.8±10.50	4.87±0.08	4.44±0.08	96.97	97.24	0.30	0.30
2	As	0.35±0.0001	-3.19	-2.81	~100	~100	0.01	0.01
3	Cu	166.05±10.30	44.25±3.99	132.81±8.15	73.35	20.01	2.00	1.00
4	Cr	153±9.41	121.62±7.99	115.56±8.01	20.51	24.47	0.05	0.05
5	Ni	135.35±8.17	28.56±2.85	20.56±0.75	78.90	84.81	0.02	0.02
6	Pb	107±7.93	15.62±1.64	31.25±0.86	85.39	70.79	0.015	0.01
7	Zn	158.49±10.12	150.26±10.06	73.44±4.05	5.20	53.67	5.0	3.00
8	Cd	163.35±10.61	126.56±8.01	128.62±7.99	22.52	21.27	0.02	1.0

EPFBB-CHB = Empty Palm Fruit Bunch Biochar-Coconut Husk Biochar. PKB-CSB = Palm Kernel Shell-Coconut Shell Biochar.

Article DOI: 10.52589/AJENSR-VZVQM4DR
DOI URL: https://doi.org/10.52589/AJENSR-VZVQM4DR

Figure 1. Treatment Performance of Two Biochar Composites for Heavy Metal Reduction in Soil

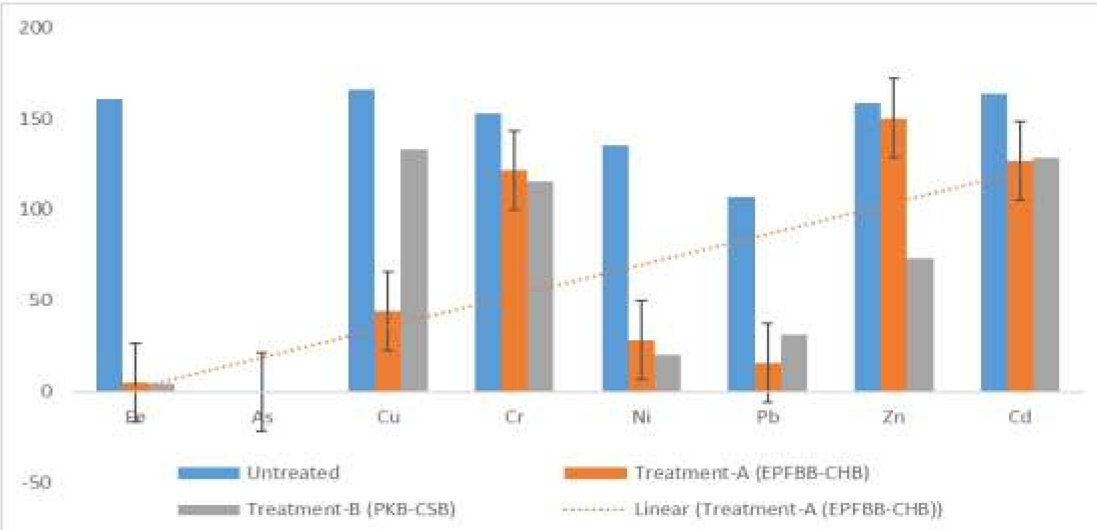

Table 2. Profile Analysis of Empty Palm Fruit Bunch Biochar (EPFB)				
S/N	**Compound**	**Formula**	**Concentration (%)**	**Key Functional Groups**
1	Thiocyanic acid, 2,4-dinitrophenyl ester	$C_7H_3N_3O_4S$	12.068	Thiocyanate (–SCN), Nitro (–NO_2)
2	2,3,4-Trimethoxy-6-nitrobenzaldehyde	$C_{10}H_{11}NO_6$	10.502	Aldehyde (–CHO), Ether (–OR), Nitro (–NO_2)
3	5-Bromo-2-(2-hydroxy-5-nitrobenzyl	$C_{14}H_8BrN_3O_3$	8.159	Imine (–C=N–), Nitrile (–C≡N), Phenol (–OH), Halide (–Br)
4	2-Methylbenzene-1,4-diamine, N1,N4-bis(heptafluorobutyryl)	$C_{15}H_8F_{14}N_2O_2$	8.569	Pyrrole rings, Carboxylic acid (–COOH)
5	2H,8H-Benzo[1,2-b:3,4-b']dipyran-6-propanoic acid, 3,9-dibromo-5-methoxy-2,2,8,8-tetramethyl	$C_{20}H_{22}Br_2O_5$	8.838	Benzopyran (chromene), Carboxylic acid, Halide (–Br)

Article DOI: 10.52589/AJENSR-VZVQM4DR
DOI URL: https://doi.org/10.52589/AJENSR-VZVQM4DR

ISSN: 2689-9434
Volume 9, Issue 3, 2026 (pp. 95-112)

6	7-Chloro-4-methoxy-3-methylquinoline	$C_{11}H_{10}ClNO$	8.587	Quinoline ring, Ether (–OCH_3), Halide (–Cl)
7	2,3,4,5,6-Pentabromobenzyl alcohol, isopropyl ether	$C_{10}H_9Br_5O$	11.260	Silyl ether (–$SiMe_3$), Ester (feruloyl bond)
8	Z,Z-6,25-Tetratriactontadien-2-one	$C_{34}H_{64}O$	10.640	Ketone (C=O), Alkenes (C=C)
9	6-Azaestra-1,3,5(10),6,8-pentaen-17-one, 3-methoxy	$C_{18}H_{19}NO_2$	11.462	Steroid backbone (with N-substitution), Ketone, Ether
10	N-(4-bromo-2-chlorophenyl)	$C_8H_7BrClNO$	9.916	Amide (–CONH–), Halides (–Br, –Cl)

Table 3: Profile Analysis of Coconut Husk Biochar (CHB)

S/N	Compound	Formula	Concentration (%)	Functional Groups
1	(2E,4E)-5-Chloro-3,4-dimethyl-2,4-heptadiene	$C_9H_{15}Cl$	11.19	Alkene (C=C), Halide (−Cl)
2	4-(Dipropylphosphoryl)-4-methylpentan-2-one	$C_{12}H_{25}O_2P$	7.83	Phosphine oxide/phosphoryl (P=O), Ketone (C=O)
3	Benzene-1,4-bis(4-formylbenzylazinomethyl)-	$C_{24}H_{18}N_4O_2$	9.81	Azine (−C=N−N=C−), Aldehyde (−CHO)
4	Fluoxymesterone	$C_20H_{29}FO_3$	14.39	Fluorine (−F), Hydroxyl (−OH), Ketone, Steroid nucleus
5	1,4-Benzodioxin, 2,3-dihydro-6-nitro-	$C_8H_7NO_4$	8.87	Benzodioxin ring, Nitro (−NO2)

Article DOI: 10.52589/AJENSR-VZVQM4DR
DOI URL: https://doi.org/10.52589/AJENSR-VZVQM4DR

6	Dichlorine monoxide	Cl_2O	10.12	Cl2O (Note: This is an inorganic covalent compound)
7	Benzeneethanamine derivative	$C_{17}H_{2}0FNO_{3}$	8.80	Aromatic ring, Amine (−NH2)
8	1-Phenyl-3-(4′-pyridyl)-propenone	$C_{14}H_{11}NO$	9.17	Enone system (−C=C−C=O), Pyridine ring
9	Quinuclidin-3-one derivative	$C_{17}H_{14}Cl_2N_2O$	9.93	Quinuclidine (bicyclic amine), Ketone
10	4′-(10-Amino-9-phenanthrylazo)acetanilide	$C_{22}H_{18}N_4O$	9.88	Azo link (−N=N−), Amide (−NH−CO−), Amine

Table 4: Profile Analysis of Palm Kernel Shell Biochar (PKSB)

S/N	**Compound**	**Formula**		**Concentration (%)**	**Key Functional Groups**
1	2-[4-(1-oxo-3-phenyl-2-propenyl)phenyloxy]	$C_{17}H_{15}NO_3$		9.460	Secondary Amide, Enone (C=C−C=O), Phenoxy Ether
2	2H,8H-Benzo[1,2-b:3,4-b']dipyran-6-propanoic acid, 3,9-dibromo-5-methoxy-2,2,8,8-tetramethyl	$C_{20}H_{22}Br_2O_5$		10.669	Benzopyran (chromene), Carboxylic acid, Halide (−Br), Ether
3	4-Pyridinol, 2,6-bis[p-bromophenyl]-3,5-dichloro	$C_{17}H_9Br_2Cl_2NO$		10.759	Pyridine ring, Phenol (−OH), Halides (−Cl,−Br)
4	6-Chloro-N,N-dimethyl-2,1,3-benzoxadiazol-4-amin	$C_8H_8ClN_3O$		10.657	Benzoxadiazole ring, Tertiary Amine, Halide (−Cl)
5	Propenone, 3-(4-chlorophenyl)-1-[5-(3-	$C_{18}H_{15}ClO_2S$		10.058	Thiophene ring, Enone, Alkyne

Article DOI: 10.52589/AJENSR-VZVQM4DR
DOI URL: https://doi.org/10.52589/AJENSR-VZVQM4DR

	hydroxy-3-methyl-1-butynyl)-2-thienyl]				(C≡C), Alcohol, Halide
6	N-(cyclohexylcarbonyl)-, pentadecyl ester	$C_{25}H_{47}NO_3$		11.514	Tertiary Amide, Long-chain Ester (Aliphatic)
7	15,17,19,21-Hexatriacontatetrayne	$C_{36}H_{58}$		9.168	Four conjugated Triple Bonds (C≡C×4), Aliphatic
8	Spiro(1,3-dithiane)-2,16'-(androst-5'-ene-3',17'-diol), diacetate	$C_{26}H_{38}O_4S_2$		8.925	Steroid backbone, Dithiane ring (S-heterocycle), Ester
9	1,2-Bis[1-(2-hydroxyethyl)-3,6-diazahomoadamantantydene-9]hydrazine	$C_{22}H_{36}N_6O_2$		9.350	Homoadamantane (Aza-adamantane), Hydrazine (−N−N−), Alcohol
10	1H-2-benzopyran-1,3(4H)-dione, 4-[2-(3-ethyl-2(3H)-benzoxazolylidene)ethylidene]	$C_{20}H_{15}NO_4$		9.442	Benzopyran-dione, Benzothiazole ring, Conjugated Polyene

Table 5: Profile Analysis of Coconut Shell Biochar (CSB)

S/N	Compound	Formula	Concentration (%)	Key Functional Groups
1	Phosphine, 2,5-furandiylbis [dipheny	$C_{28}H_{22}OP_2$	10.420	Phosphine (−PPh2), Furan ring
2	4-Bromo-1-(1,1,3-trichloropropan-2-yl) pyrazole	$C_6H_6BrCl_3N_2$	6.797	Pyrazole ring, Halides (−Br,−Cl)
3	1,2,5-Oxadiazol-3-amine, 4-[5-(3-pyridinyl)-1H-1,2,3-triazol-1-yl]	$C_9H_7N_7O$	7.375	Oxadiazole, Triazole, Pyridine, Primary Amine
4	1-Androsten-3,17-dione, di-trimethylsilyl	$C_{25}H_{42}O_2Si_2$	7.816	Steroid nucleus, Silyl ether (−SiMe3), Enone

Article DOI: 10.52589/AJENSR-VZVQM4DR
DOI URL: https://doi.org/10.52589/AJENSR-VZVQM4DR

5	Ethyl 3-methyl-8-[p-sulfamylbenzylamino] pyrido[2,3-b] pyrazin-6-carbamate	$C_{18}H_{2}0N_{6}O_{4}S$	7.614	Carbamate (−NHCOOR), Sulfonamide, Pyrido-pyrazine
6	1(3H)-isobenzofuranone, 4,5,6-trimethoxy	$C_{11}H_{12}O_{5}$	8.912	Phthalide (cyclic ester), Methoxy ethers (−OCH3)
7	benzaldehyde 4-[2-pyridyl]-3-thiosemicarbazone	$C_{13}H_{12}N_{4}S$	6.934	Thiosemicarbazone (−C=N−NH−CS−NH2), Pyridine
8	Hexasiloxane, 1,1,3,3,5,5,7,7,9,9,11,11-dodecamethyl	$C_{12}H_{38}O_{5}Si_{6}$	8.884	Siloxane chain (−Si−O−Si−), Methyl groups
9	Phenol, 2-[4-(2-hydroxyethylamino)-2-quinazolinyl]	$C_{16}H_{15}N_{3}O_{2}$	13.779	Quinazoline ring, Phenol (−OH), Secondary Amine
10	Octasiloxane, 1,1,3,3,5,5,7,7,9,9,11,11,13,13,15,15-hexadecamethyl	$C_{16}H_{5}0O_{7}Si_{8}$	21.468	Linear Siloxane polymer, Methyl groups

Table 6: Summary of Results for Biochar Samples

S/N	**Parameter(s)**	**CH**	**CS**	**PKS**	**EPFB**
1	Ash Content (%)	57.416	44.657	34.890	50.449
2	CEC (meq/100g)	107.831	40.084	29.996	94.537
3	Porosity (%)	64	48	42	60
4	Fixed Carbon (%)	65.20	53.65	47.89	60.51
5	Surface Area (m^2/g)	10	8	7	12

Article DOI: 10.52589/AJENSR-VZVQM4DR
DOI URL: https://doi.org/10.52589/AJENSR-VZVQM4DR

Figure 2. Surface Physicochemistry of Four Different Biochars Used for Heavy Metals Adsorption

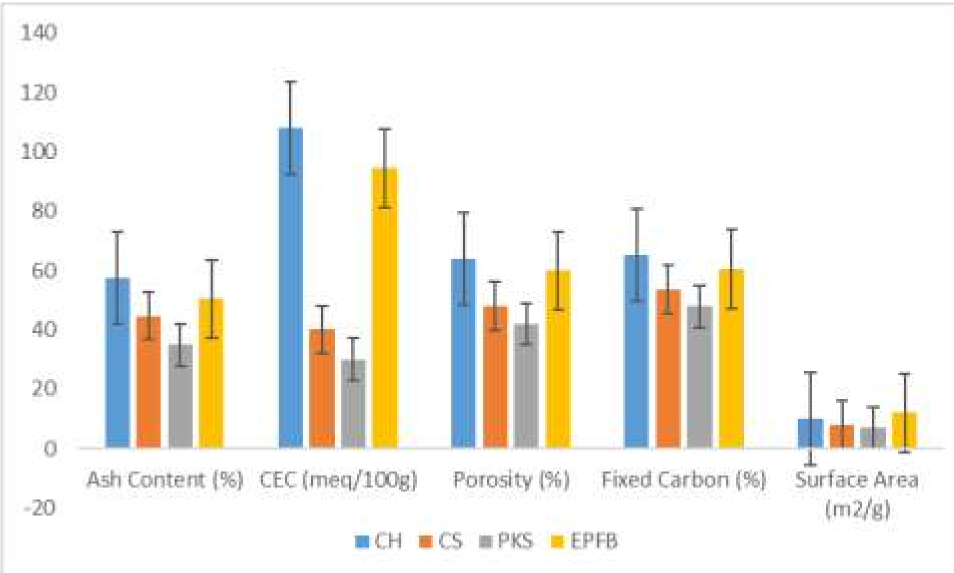

DISCUSSION

Heavy Metal Contamination Status and Remediation Performance

From the results in Table 1, iron (Fe) concentration in the untreated soil was 160.8 ± 10.50 mg/L, far exceeding the regulatory limits of 0.30 mg/L set by USEPA (2022) and SON (2015). Application of EPFBB-CHB reduced Fe concentration to 4.87 ± 0.08 mg/L, while PKB-CSB further reduced it to 4.44 ± 0.08 mg/L. These values correspond to removal efficiencies of approximately 97.0% and 97.2%, respectively. Although the treated concentrations remained marginally above permissible limits, the level of reduction demonstrates strong Fe retention by both biochar composites. This high affinity may be attributed to their porous structure, extensive surface area, and abundance of oxygenated functional groups that promote adsorption and surface complexation. These findings align with Wang et al. (2023), who reported a 99.9% Fe removal efficiency using magnetic biochar composites derived from Fenton sludge and carboxymethyl cellulose, achieving an adsorption capacity of 199.9 mg/g.

Copper (Cu) concentration in untreated soil measured 166.05 ± 10.30 mg/L, exceeding USEPA (2022) (2.00 mg/L) and SON (2015) (1.00 mg/L) limits. Following remediation, EPFBB-CHB reduced Cu to 44.25 ± 3.99 mg/L, representing a 73.34% reduction, while PKB-CSB achieved a lesser reduction to 132.81 ± 8.15 mg/L, corresponding to 20.05%. The superior removal efficiency of EPFBB-CHB suggests enhanced Cu-binding capacity through ion exchange and surface complexation mechanisms. These findings are comparable with Yan et al. (2020), who reported Cu removal of 34.1 mg/g using hydrous ferric oxide-modified biochar, but contrast with Jia et

Article DOI: 10.52589/AJENSR-VZVQM4DR
DOI URL: https://doi.org/10.52589/AJENSR-VZVQM4DR

ISSN: 2689-9434
Volume 9, Issue 3, 2026 (pp. 95-112)

al. (2022), who reduced Cu concentration to 0.1273 ppm using optimized biochar feedstocks under controlled conditions.

Chromium (Cr) contamination was high, with untreated soil observed to be 153 ± 9.41 mg/L, far exceeding the USEPA (2022) regulatory limit of 0.05 mg/L. Treatment with EPFBB-CHB reduced Cr concentration to 121.62 ± 7.99 mg/L, while PKB-CSB achieved 115.56 ± 8.01 mg/L, corresponding to removal efficiencies of 20.6% and 24.5%, respectively. These results demonstrate moderate Cr immobilization, likely influenced by chromium's complex redox chemistry and lower bioavailability. The findings correspond with Jia et al. (2022), who reduced Cr from 10 mg/L to 0.538 mg/L, but are substantially lower than the 99.57% removal reported by Hina et al. (2023) using sugarcane bagasse- and citrus peel-derived biochars.

Nickel (Ni) concentration in untreated soil was 135.35 ± 8.17 mg/L, significantly exceeding the USEPA (2022) and SON (2015) threshold of 0.02 mg/L. Treatment with EPFBB-CHB reduced Ni to 28.56 ± 2.85 mg/L, representing a 78.9% reduction, while PKB-CSB further reduced it to 20.56 ± 0.75 mg/L, achieving 84.8% removal. The enhanced performance of PKB-CSB may be attributed to higher porosity and greater availability of active adsorption sites. These findings closely align with Tichem et al. (2023), who reported Ni removal efficiencies of 99.80–99.96% using iron-modified rice husk biochar, and exceed the 57.2% reported by Huang et al. (2022) using modified coconut shell biochar.

Lead (Pb) contamination was severe, with untreated soil recording 107 ± 7.93 mg/L, far exceeding the permissible limits of 0.015 mg/L (USEPA) (2022) and 0.01 mg/L (SON) (2015). EPFBB-CHB reduced Pb concentration to 15.62 ± 1.64 mg/L, achieving an 85.4% reduction, while PKB-CSB reduced it to 31.25 ± 0.86 mg/L, corresponding to 70.8%. The stronger Pb immobilization by EPFBB-CHB may be linked to its higher cation exchange capacity and pore connectivity. These results are consistent with Hina et al. (2023), who reported 99.59% Pb removal using biochars derived from urban biowaste, but contrast Shafiq et al. (2023), who achieved only 47.63% removal using ZnMgAl-LDH–rice husk biochar composites.

Zinc (Zn) concentration in untreated soil was 158.495 ± 10.12 mg/L, exceeding USEPA (5.0 mg/L) and SON (3.0 mg/L) standards. EPFBB-CHB achieved a marginal reduction to 150.26 ± 10.06 mg/L (5.3%), whereas PKB-CSB reduced Zn substantially to 73.44 ± 4.05 mg/L, representing a 53.7% reduction. These findings align with Huang et al. (2022), who reported a 12.7% Zn reduction, but contrast Ahsan et al. (2024) and Jia et al. (2022), who achieved over 95% removal under optimized conditions.

Cadmium (Cd) concentration in untreated soil was 163.35 ± 10.61 mg/L, exceeding USEPA (2022) (0.02 mg/L), SON (2015) (1.0 mg/L), intervention limits. EPFBB-CHB reduced Cd to 126.56 ± 8.01 mg/L (22.5%), while PKB-CSB reduced it to 128.62 ± 7.99 mg/L (21.3%). These reductions align with Huang et al. (2022) but are lower than the 89.87% reported by Khan et al. (2019).

Arsenic in the untreated soil (0.35 ± 0.0001 mg/L) far exceeded USEPA/SON limits (0.01 mg/L). Treatment with biochar composites reduced it below regulatory thresholds, with EPFBB-CHB removing 3.19 mg/L and PKB-CSB removing 2.81 mg/L. EPFBB-CHB's higher efficacy (13.5%)

Article DOI: 10.52589/AJENSR-VZVQM4DR
DOI URL: https://doi.org/10.52589/AJENSR-VZVQM4DR

may be due to greater surface area, porosity, and functional groups, enabling adsorption, complexation, and immobilization of arsenic from soil matrices.

One-way analysis of variance (ANOVA) was conducted to determine whether the application of biochar composites significantly affected heavy metal concentrations in contaminated soil. The ANOVA results showed an F value of 2.10 with a corresponding p-value of 0.151 at a 95% confidence level. The null hypothesis (assuming no difference in treatment performance was not rejected since the p-value (0.151) > 0.05 and the F value (2.10) < (3.55).

This result indicates that there was no statistically significant difference between soil treated with EPFBB–CHB biochar composite and soil treated with PKB–CSB biochar composite. The lack of statistical significance may be attributed to variability within the data or the limited number of observations used in the analysis.

Despite the absence of statistical significance, the descriptive results still suggest that the application of agro-waste biochar composites contributed to a reduction in heavy metal concentrations in the contaminated soil. This indicates that the biochar materials possess adsorption and immobilization properties capable of reducing the mobility of heavy metals in soil systems.

Influence of Biochar Physicochemical Properties

The remediation performance observed in Table 1 was observed to be strongly supported by the physicochemical characteristics of the biochar presented in Table 6. EPFB biochar exhibited the highest surface area (12 m^2/g) and substantial porosity (60%), while CH biochar demonstrated the highest cation exchange capacity (107.831 meq/100 g) and porosity (64%). According to Zeng et al. (2022), elevated surface area enhances adsorption through increased availability of binding sites, whereas high porosity facilitates diffusion of metal ions into internal pore networks.

Cation exchange capacity plays a central role in immobilizing divalent and trivalent metal cations through electrostatic attraction and ion exchange mechanisms. The relatively high CEC values of EPFB (94.537 meq/100 g) and CH explain the strong immobilization of Pb^{2+}, Cu^{2+}, Ni^{2+}, and Fe^{2+}/Fe^{3+}. The comparatively moderate removal of Cr and Cd may be linked to chromium's redox-sensitive speciation and cadmium's weaker complexation affinity under near-neutral conditions (Liu et al., 2023). Furthermore, the high fixed carbon contents (65.20% for CH and 60.51% for EPFB) indicate enhanced aromaticity and structural stability, which contribute to long-term sorption capacity.

A one-way analysis of variance (ANOVA) was performed to evaluate the significance of variations in the physicochemical properties across the four biochar types: coconut husk (CH), coconut shell (CS), palm kernel shell (PKS), and empty palm fruit bunch (EPFB). The analysis yielded an F-statistic of 0.97 with a corresponding p-value of 0.438 ($p > 0.05$) at a 95% confidence level. Given that the calculated F-value remained below the critical threshold ($F_{crit} = 3.49$), the null hypothesis was retained, indicating no statistically significant differences in the primary physicochemical characteristics among the feedstocks.

Article DOI: 10.52589/AJENSR-VZVQM4DR
DOI URL: https://doi.org/10.52589/AJENSR-VZVQM4DR

However, descriptive data highlighted localized performance trends. CH biochar demonstrated the highest cation exchange capacity (CEC) and porosity, attributes which are fundamentally linked to the enhanced adsorption of metallic cations in contaminated soil matrices. Furthermore, EPFB biochar exhibited the most extensive surface area, suggesting a superior density of active sites available for metal immobilization. These structural characteristics are instrumental in driving remediation mechanisms such as ion exchange, surface complexation, and intra-particle pore diffusion.

The observed homogeneity in biochar properties likely stems from the similar lignocellulosic profiles of the precursor agro-wastes and the application of standardized pyrolysis parameters during thermal conversion. Consequently, the results suggest that all four biochar variants possess the requisite structural integrity and functional properties to effectively mitigate heavy metal mobility in environmental remediation applications.

Role of Feedstock Composition and Surface Functional Groups

Analyses of EPFB, CH, PKS, and CS (Tables 2–5) revealed diverse organic constituents, including aromatic hydrocarbons, phenolic derivatives, nitrogen-containing heterocycles, and oxygenated compounds. Although pyrolysis at 500 °C alters the original chemical structures, such precursor molecules influence the formation of stable aromatic carbon frameworks enriched with functional groups such as hydroxyl, carboxyl, and carbonyl moieties (Kwang et al., 2012). These oxygen containing groups are widely recognized as critical for heavy metal binding through surface complexation and coordination reactions (Yang et al., 2019).

Additionally, the relatively high ash contents of CH (57.416%) and EPFB (50.449%) suggest the presence of mineral phases capable of facilitating precipitation and co-precipitation mechanisms, particularly for Fe and Pb. Mineral components may promote the formation of insoluble metal complexes, thereby reducing bioavailability. The variation in compound profiles among EPFB, CH, PKS, and CS likely contributed to differences in pore development, surface chemistry, and ultimately adsorption performance observed between EPFBB–CHB and PKB–CSB composites.

The results of this study revealed that heavy metal immobilization occurred through multiple interacting mechanisms, including ion exchange, electrostatic attraction, surface adsorption, complexation with oxygenated functional groups, and mineral precipitation. The superior performance of EPFBB–CHB for Fe, Cu, Pb, and Ni reflects its favorable surface area and exchange capacity, whereas PKB–CSB enhanced Zn and Cr removal suggests metal-specific interactions influenced by its structural composition.

Ferrali et al. (2001) observed that the presence of benzopyrone compounds (Tables 2 and 4) contributes to structures that act as potent iron-chelating agents. These compounds form stable 2:1 complexes with divalent and trivalent metal ions such as Fe, Cu, and Zn, making them valuable for both biological and environmental metal removal applications. Similarly, thiosemicarbazones, including benzaldehyde 4-[2-pyridyl]-3-thiosemicarbazone (Table 5), and their derivatives are highly effective chelating agents. They exhibit strong coordination tendencies, enabling the formation of stable metal complexes, enhanced selectivity, and a propensity to form macrocyclic ligands (Aly et al., 2023).

Article DOI: 10.52589/AJENSR-VZVQM4DR
DOI URL: https://doi.org/10.52589/AJENSR-VZVQM4DR

The presence of sulfur and nitrogen donor atoms enables biochars to form stable complexes with divalent metal ions such as cadmium (Cd), nickel (Ni), copper (Cu), and cobalt (Co) (Hashmi et al., 2025). This property is widely exploited in bioremediation and chemical precipitation processes for the removal of heavy metals from wastewater and contaminated soils. Zhang et al. (2020) successfully utilized mango peel, a common agricultural waste, for the removal of cadmium (Cd^{2+}) from aqueous solutions, achieving an adsorption efficiency of 67.7%. The study also reported the presence of oxygen-containing functional groups, such as carboxyl and hydroxyl groups, which played a critical role in facilitating chemical interactions with metal ions and enhancing their adsorption from environmental matrices.

This study revealed that despite substantial diminutions, residual metal concentrations remained above regulatory standards. Target environmental levels could be achieved via repeated treatment cycles, increased treatment dose, optimization strategies, and chemical modification. Nevertheless, the results support growing evidence that agro-waste biochar represents a viable and sustainable approach for reducing heavy metal mobility in contaminated tropical soils (Tian et al., 2025).

CONCLUSION

The remediation efficiency of the two biochar composites was evaluated by calculating the percentage reduction in heavy metal concentrations relative to the untreated soil. The study findings indicated that agro-waste biochar composites markedly reduced heavy metal concentrations in heavy metal-contaminated soils. The untreated soil exhibited significantly elevated contamination levels, with Fe at 160.8 ± 10.50 mg/L, Cu at 166.05 ± 10.30 mg/L, Cr at 153 ± 9.41 mg/L, Ni at 135.35 ± 8.17 mg/L, Pb at 107 ± 7.93 mg/L, Zn at 158.495 ± 10.12 mg/L, Cd at 163.35 ± 10.61 mg/L, and As at 0.35 ± 0.0001 mg/L (unspiked environmental concentration). Treatment-B (PKB-CSB) demonstrated slightly higher efficiency in removing Fe, Cr, Ni, and Zn, with removal efficiencies of 97.24%, 24.47%, 84.81%, and 53.67%, respectively. In contrast, Treatment-A (EPFBB-CHB) exhibited greater effectiveness in the removal of Cu, Pb, and Cd, achieving removal efficiencies of 73.35%, 85.39%, and 22.52%, respectively.

Both treatments showed complete immobilization of arsenic, as concentrations were reduced to below detectable levels after treatment, indicating 100% remediation performance of these composites at environmental contamination concentrations. These findings also reveal that the adsorption performance of the biochar composites varies depending on the type of metal present, which may be attributed to differences in the physicochemical properties and surface functional groups of the biochar.

The study further established that biochar physicochemical properties, including surface area, porosity, cation exchange capacity, and ash content, coupled with functional groups derived from feedstock composition, were key determinants of metal immobilization. GC–MS analysis revealed the presence of aromatic, phenolic, nitrogenous, and oxygenated compounds in the feedstocks, which contributed to the formation of stable, metal-binding biochar structures during pyrolysis. Mechanistically, immobilization occurred through a combination of ion exchange, surface adsorption, complexation, and mineral precipitation.

Article DOI: 10.52589/AJENSR-VZVQM4DR
DOI URL: https://doi.org/10.52589/AJENSR-VZVQM4DR

Generally, the findings indicate that agro-waste biochar composites represent a cost-effective and sustainable approach for mitigating heavy metal mobility in petroleum-impacted soils. To achieve compliance with regulatory limits, optimization through increased application rates, chemical activation, or repeated treatments may be required.

REFERENCES

Abbas, F., Hammad, H. M., Anwar, F., Farooque, A. A., Jawad, R., Bakhat, H. F., Naeem, M. A., Ahmad, S., & Qaisrani, S. A. (2021). Transforming a valuable bioresource to biochar, its environmental importance, and potential applications in boosting circular bioeconomy while promoting sustainable agriculture. *Sustainability, 13*(1), 1–15.

Ahmed, M. S., Pant, R. R., Alao, J. O., Chaurasia, P. K., Abdelkebir, B., & Abd-Elmaboud, M. E. (2025). Soil remediation through washing and flushing: Bibliometric trends and future prospects. *Environmental Earth Sciences, 401*, 1–16.

Aly, A. A., Abdallah, E. M., Ahmed, S. A., Rabee, M. M., & Bräse, S. (2023). Transition metal complexes of thiosemicarbazides, thiocarbohydrazides, and their corresponding carbazones with Cu(I), Cu(II), Co(II), Ni(II), Pd(II), and Ag(I)—A review. *Molecules, 28*(4), 1808. https://doi.org/10.3390/molecules28041808

Ezugwu, B. U., Bala, J. D., Abioye, O. P., & Oyewole, O. A. (2022). Effects of petroleum pollution and the remediation attempts in Ogoniland, Rivers State, Nigeria: A review. *Nigerian Journal of Microbiology, 36*(1), 6081–6101.

Ferrali, M., Donati, D., Bambagioni, S., Fontani, M., Giorgi, G., & Pietrangelo, A. (2001). 3-Hydroxy-(4H)-benzopyran-4-ones as potential iron chelating agents in vivo. *Bioorganic & Medicinal Chemistry, 9*(11), 3041–3047. https://doi.org/10.1016/S0968-0896(01)00207-3

Hashmi, K., Satya, Mishra, P., Veg, E., Khan, T., & Joshi, S. (2025). Computational studies of thiosemicarbazone-based metal complexes and their biological applications. *Engineering Proceedings, 117*(1), Article 23. https://doi.org/10.3390/engproc2025117023

Hina, C., J., Dinakaran, J., Tenzen, N., Krati, V., & K.S., R. (2023). Comparison of adsorption performance of biochar derived from urban biowaste materials for removal of heavy metals. *Environmental Management, 1*, 1–17. https://doi.org/10.1007/s00267-023-01866-1

Huang, A., Bai, W., Yang, S., Wang, Z., Wu, N., Zhang, Y., & Li, D. (2022). Adsorption characteristics of chitosan-modified bamboo biochar in Cd(II)-contaminated water. *Journal of Chemistry, 2022*(1), 6–12.

Jia, L., Hao, W., Nan, M., Beihai, Z., Huilun, C., & Rongfang, Y. (2022). Optimization of the raw materials of biochars for the adsorption of heavy metal ions from aqueous solution. *Water Science & Technology, 85*, 2869–2881. https://doi.org/10.2166/wst.2022.158

Khan Agha, S., Priyatharshini, S., Dhevagi, P., Chitdeshwari, T., & Avudainayagam, S. (2019). Removal of lead and cadmium from aqueous solutions by banana peel biochar. *Madras Agricultural Journal, 106*, 45–53.

Kwang, H.K., Jae-Young, K., Tae-Su, C., Joon Weon, C. (2012). Influence of pyrolysis temperature on physicochemical properties of biochar obtained from the fast pyrolysis of pitch pine (Pinus rigida). *Bioresource Technology, 118*, 158- 162.

Article DOI: 10.52589/AJENSR-VZVQM4DR
DOI URL: https://doi.org/10.52589/AJENSR-VZVQM4DR

Liu, B., Xin, Y.-N., Zou, J., Khoso, F. M., Liu, Y.-P., Jiang, X.-Y., Peng, S., & Yu, J.-G. (2023). Removal of chromium species by adsorption: Fundamental principles, newly developed adsorbents and future perspectives. *Molecules, 28*(2), 639. https://doi.org/10.3390/molecules28020639

Mahmoud, E.R.I., Aly, H.M., Hassan, N.A., Aljabri, A., Khan, A.L., & El-Labban, H.F. (2024). Biochar from date palm waste via two-step pyrolysis: A modified approach for Cu(II) removal from aqueous solutions. Processes, 12, 1–19. https://doi.org/10.3390/pr12061189

Mohan, D., Sarswat, A., Ok, Y.S., & Pittman, C.U. (2014). Organic and inorganic contaminants removal from water with biochar, a renewable, low-cost and sustainable adsorbent—A critical review. *Bioresource Technology, 160*, 191–202.

Onwuchekwa, D. (2022). The application of linear programming in the agricultural sector: A study of Songhai Farm, Bunu, Tai Local Government Area of Rivers State. *Journal of Accounting, Marketing and Management Research, 9*(2), 24-30.

Shafiq, M., Alazba, A.A., & Amin, M.T. (2023). Preparation of ZnMgAl-layered double hydroxide and rice husk biochar composites for Cu(II) and Pb(II) ions removal from synthetic wastewater. *Water, 15*, 1–17. https://doi.org/10.3390/w15122207

Sizmur, T., Fresno, T., Akgül, G., Frost, H., & Moreno-Jiménez, E. (2017). Biochar modification to enhance sorption of inorganics from water. *Bioresource Technology, 246*, 34–47.

Tian, F., Wang, Y., Zhao, Y., Sun, R., Qi, M., Wu, S., & Wang, L. (2025). A review of biochar–industrial waste composites for sustainable soil amendment: Mechanisms and perspectives. *Water, 17*(1), 1–27.

Tichem, T.M., Wang, Y., Gameli, R.B.H., Mbage, B., & Li, B. (2023). Multicomponent adsorption of pollutants from wastewater using low-cost eco-friendly iron-modified rice husk biochar in the era of green chemistry. *Sustainability, 15,* 1–14. https://doi.org/10.3390/su152316348

United Nations Environment Programme (UNEP). (2011). Environmental Assessment of Ogoniland. United Nations. https://postconflict.unep.ch/publications/OEA/UNEP_OEA.pdf

United States Environmental Protection Agency (USEPA). (2022). Metals Cooperative Research and Development Agreement (CRADA) phase I report: Development of an overarching bioavailability modeling approach to support US EPA's Aquatic Life Water Quality Criteria for Metals (EPA-822-R-22-001). EPA Office of Water.

Wang, Z., Guo, J., Jia, J., Liu, W., Yao, X., Feng, J., Dong, S., & Sun, J. (2023). Magnetic biochar derived from Fenton sludge/CMC for high-efficiency removal of Pb(II): Synthesis, application, and mechanism. *Molecules, 28,* 1-5. https://doi.org/10.3390/molecules28134983

Yaashikaa, P.R., Kumar, P.S., Varjani, S., & Saravanan, A. (2020). A critical review on the biochar production techniques, characterization, stability and applications for circular bioeconomy. *Biotechnology Reports, 28*, 1-5.

Yan, L., Liangmin, G., Zhongxiang, L., Yuchen, W., Yan, W., & Shunli, W. (2020). Enhanced removal of heavy metals from water by hydrous ferric oxide-modified biochar. *ACS Omega, 5,* 28702–28711. https://dx.doi.org/10.1021/acsomega.0c03893

Yang, X., Wan, Y., Zheng, Y., He, F., Yu, Z., Huang, J., Wang, H., Ok, Y. S., Jiang, Y., & Gao, B. (2019). Surface functional groups of carbon-based adsorbents and their roles in the removal of heavy metals from aqueous solutions: A critical review. *Chemical Engineering Journal, 366*, 608–621. https://doi.org/10.1016/j.cej.2019.02.119

Zeng, X., Zhang, G., Zhu, J., & Wu, Z. (2022). Adsorption of heavy metal ions in water by surface functionalized magnetic composites: A review. Environmental Science. *Water Research & Technology, 5*,8(907–925). https://doi.org/10.1039/D1EW00868D

Zhang, P., Yang, M., Lan, J., Huang, Y., Zhang, J., Huang, S., Yang, Y., & Ru, J. (2023). Water quality degradation due to heavy metal contamination: Health impacts and eco-friendly approaches for heavy metal remediation. *Toxics, 11*(10), 1–20. https://doi.org/10.3390/toxics11100828

Zhang, L., Ren, Y., Xue, Y., Cui, Z., Wei, Q., Han, C., & He, J. (2020). Preparation of biochar by mango peel and its adsorption characteristics of Cd(II) in solution. *RSC Advances, 10*(59), 35878–35888. https://doi.org/10.1039/D0RA06586B

Article DOI: 10.52589/AJENSR-VZVQM4DR
DOI URL: https://doi.org/10.52589/AJENSR-VZVQM4DR